MASTER

μ- AND τ-PAIR PRODUCTION FROM RELATIVISTIC HEAVY-ION COLLISIONS*

C. Bottcher and M. R. Strayer

Physics Division
Oak Ridge National Laboratory
Oak Ridge, Tennessee 37831

CONF-8606183--2

DE86 014221

presented at

NATO International Advanced Course on
Physics of Strong Fields

Maratea, Italy

June 1-14, 1986

DISCLAIMER

This report was prepared as an account of work sponsored by an agency of the United States Government. Neither the United States Government nor any agency thereof, nor any of their employees, makes any warranty, express or implied, or assumes any legal liability or responsibility for the accuracy, completeness, or usefulness of any information, apparatus, product, or process disclosed, or represents that its use would not infringe privately owned rights. Reference herein to any specific commercial product, process, or service by trade name, trademark, manufacturer, or otherwise does not necessarily constitute or imply its endorsement, recommendation, or favoring by the United States Government or any agency thereof. The views and opinions of authors expressed herein do not necessarily state or reflect those of the United States Government or any agency thereof.

*Research sponsored by the U.S. Department of Energy under contract DE-AC05-840R21400 with Martin Marietta Energy Systems, Inc.

DISTRIBUTION OF THIS DOCUMENT IS UNLIMITED

μ- AND τ-PAIR PRODUCTION FROM RELATIVISTIC HEAVY-ION COLLISIONS*

C. Bottcher and M. R. Strayer

Physics Division
Oak Ridge National Laboratory
Oak Ridge, Tennessee 37831

INTRODUCTION

In these lectures we shall attempt to address the question of μ- and τ-pair production from the motional Coulomb fields available at the new relativistic heavy-ion accelerators. It is well known that electrons and positrons are produced from such collisions in sizeable multiplicities,[1] and Gould[2] has suggested that heavy lepton pair creation may be possible at RHIC.

We shall divide our discussion of these phenomena into two parts. In the first part, a semiclassical field theory is developed which is appropriate for families of leptons which are coupled electromagnetically. The field equations are mapped on to a lattice of collocation points using basis spline methods, and techniques for solving the resulting lattice equations are outlined.

In the second part, we shall examine the properties of the transverse electromagnetic field near the heavy-ion beam and present physical arguments as to the feasibility of pair creation under a variety of circumstances. Using the Dirac-Hartree equations developed in part one, we shall dynamically evolve the vacuum, using the appropriate fields, and compute μ-pair and τ-pair production cross sections.

SEMICLASSICAL FIELD THEORY

In a pedagogical sense, our treatment of pair production in the presence of strong fields is similar to the early version of the adiabatic basis method developed by Greiner and co-workers.[3] However, there are important differences which we shall note in the following discussion. A more complete account of the method is given in Ref. 4. The Dirac-Hartree

*Research sponsored by the U.S. Department of Energy under contract DE-AC05-84OR21400 with Martin Marietta Energy Systems, Inc.

field equations can be obtained from three principal assumptions: i) existence of a semiclassical action and an effective Lagrangian, ii) identification of the initial state and the vacuum state, and iii) unitary time-evolution of these states.

(i) Assuming a minimal electromagnetic coupling of electrons, muons, and tauons through a classical electromagnetic field, the effective Lagrangian density case can be written as[5]

$$\mathscr{L}(x) = \mathscr{L}_e + \mathscr{L}_\mu + \mathscr{L}_\tau - 1/4\, F_{\mu\nu}F^{\mu\nu} + J_\mu A^\mu \qquad (1)$$

where, in Eq. (1), J_μ is a conserved classical external current, A^μ and $F^{\mu\nu}$ are respectively the four-vector and field tensor of the classical electromagnetic field, and where the terms $\mathscr{L}_\ell$ are given by

$$\mathscr{L}_\ell(x) = \bar{\psi}_\ell(x)\left[\gamma_\mu\left(i\partial^\mu - A^\mu\right) - m_\ell\right]\psi_\ell(x), \quad \ell = e,\mu,\tau. \qquad (2)$$

We note that this Lagrangian separately conserves electron, muon, and tauon numbers, as illustrated by the diagram in Fig. 1. Thus, the different terms in Eq. (1) are only coupled through A^μ, and we shall assume, for simplicity, that this coupling can be ignored. Thus, for each species of lepton we take[6]

$$S_\ell = \int d^4x\ {}_\ell\langle\Phi(t)\,|\,:\mathscr{L}(x):\,|\,\Phi(t)\rangle_\ell \qquad (3)$$

where $|\,\Phi(t)\rangle$ denotes the many-lepton state at a time t which evolves from the initial state, and where the normal ordering is with respect to a reference state which must be specified. This form of the action has been extensively used in nuclear physics to obtain Hartree-Fock-Bogoliubov equations.[7] In Eq. (3) the dynamical coordinates which are varied to make the action stationary are A^μ and the parameters labeling the wavefunction are $\Phi(t)$, not the lepton field operators. Thus, in what follows, it will be convenient to work in the Schrödinger picture.

(ii) The initial state is assumed to be a single Slater determinant so that

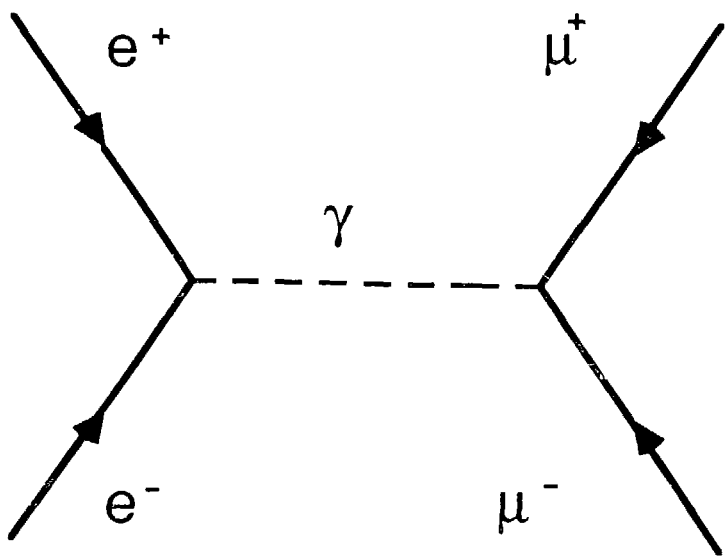

Fig. 1

$$| \psi(t)> \underset{t \to -\infty}{\to} | \phi_0 >. \tag{4}$$

We shall assume, for initial times, that there is a well-defined Dirac Hamiltonian with a spectrum as shown schematically in Fig. 2. All of the states with energies less than the label 0 are occupied in the vacuum state $| 0>$, which we shall identify as the reference state. The single-particle states with labels between 0 and f will comprise the initial state $| \Phi_0>$. By construction, the single-particle states in Fig. 2 are complete and orthonormal

$$1 = \sum_{\lambda} \{ | \chi_{\lambda}^{(+)}><\chi_{\lambda}^{(+)} | + | \chi_{\lambda}^{(-)}><\chi_{\lambda}^{(-)} | \},$$

$$\text{and} \quad <\chi_{\lambda}^{(s)} | \chi_{\lambda'}^{(s')}> = \delta_{\lambda\lambda'}\delta_{ss'} \tag{5}$$

With the choice of reference state as given above, we can identify $| \psi_{\lambda}^{(+)}>$ and $| \chi_{\lambda}^{(-)}>$ as single-particle and single anti-particle wavefunctions. In the second quantized representation, we have particle and anti-particle annihilation operators a_λ and b_λ respectively so that

$$a_\lambda | 0> = b_\lambda | 0> = 0$$

and

$$\{a_\lambda, a_{\lambda'}^{\dagger}\} = \{b_\lambda^{\dagger}, b_{\lambda'}\} = \delta_{\lambda\lambda'}. \tag{6}$$

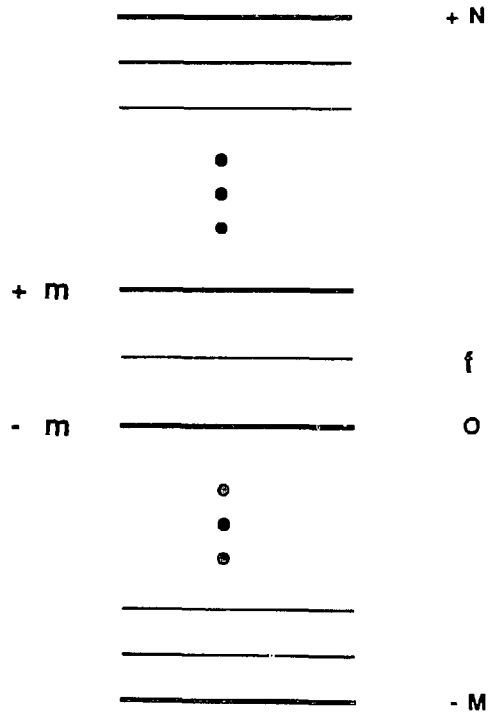

Fig. 2

All anticommutation combinations of the operators a and b not given in Eq. (6) are zero, and the initial state is

$$| \Phi_o \rangle = \prod_{0<\lambda<f} a_\lambda^\dagger | 0 \rangle. \tag{7}$$

(iii) We assume that the dynamics governing the time evolution of the wavefunction in Eq. (4) is unitary; that is

$$| \Phi(t) \rangle = S(t) | \Phi_o \rangle, \tag{8}$$

where $S^\dagger S = SS^\dagger = 1$. There are several important consequences of this assumption. Equations (7) and (8) together guarantee that the state $\Phi(t)$ is at all times a single Slater determinant. This may be seen from the following equation

$$| \Phi(t) \rangle = S(t) a_1^\dagger a_2^\dagger \ldots a_f^\dagger | 0 \rangle \tag{9}$$

By inserting $S(t)^\dagger S(t)$ between adjacent operators in the above, we can rewrite $\Phi(t)$ as

$$| \Phi(t) \rangle = \alpha_1^\dagger(t) \alpha_2^\dagger(t) \ldots \alpha_f^\dagger(t) | 0(t) \rangle \tag{10}$$

where the operators $\alpha_\lambda^\dagger(t)$ and the state $0(t)$ are given by

$$\alpha_\lambda^\dagger(t) = S(t) a_\lambda^\dagger S^\dagger(t), \qquad \lambda > 0, \tag{11}$$

and

$$| 0(t) \rangle = S(t) | 0 \rangle. \tag{12}$$

Equation (10) is a time-dependent Slater determinant, where $0(t)$, as given in Eq. (12), is the vacuum for the operators $\alpha_\lambda(t)$. It is easy to show that $0(t)$ is also the vacuum for operators $\beta_\lambda(t)$, defined as

$$\beta_\lambda^\dagger(t) = S(t)\, b_\lambda^\dagger S^\dagger(t), \qquad \lambda < 0, \tag{13}$$

and thus we can identify a complete and orthonormal set of one-particle states at any time t by

$$\begin{aligned} | \psi_\lambda^{(+)}(t) \rangle &= \alpha_\lambda^\dagger(t) | 0(t) \rangle \qquad \lambda > 0, \\ | \psi_\lambda^{(-)}(t) \rangle &= \beta_\lambda^\dagger(t) | 0(t) \rangle \qquad \lambda < 0. \end{aligned} \tag{14}$$

These states, and the determinant in Eq. (10), contain dynamical excitations of the vacuum through the term $0(t)$. We should like to emphasize that the one-particle states in Eq. (14) cannot be interpreted as physical-particle or anti-particle states, because of these vacuum excitations. Physical lepton or anti-lepton states can only be identified in terms of the projections of these states onto the initial states which define the particle and anti-particle spectrum.

The Dirac-Hartree equations of motion are obtained from the stationary principle for the action in Eq. (3). As previously stated, we shall work in the Schrödinger picture. Because of the normal ordering inherent in the matrix element defining the semiclassical action, we need to expand the field operators in terms of the states in Eqs. (5) and (6)

$$\Psi(x) = \sum_\lambda \psi_\lambda^{(+)}(x) a_\lambda + \psi_\lambda^{(-)}(x) b_\lambda^\dagger. \tag{15}$$

In this representation, Eq. (3) is written as

$$\begin{aligned} S_L = \int dt' \Big[& \langle \psi_j^{(+)} | L | \psi_k^{(+)} \rangle \langle \Phi_o | S(t)^\dagger : a_j^\dagger a_k : S(t) | \Phi_o \rangle \\ & + \langle \psi_j^{(+)} | L | \psi_k^{(-)} \rangle \langle \Phi_o | S(t)^\dagger : a_j^\dagger b_k^\dagger : S(t) | \Phi_o \rangle \\ & + \langle \psi_j^{(-)} | L | \psi_k^{(+)} \rangle \langle \Phi_o | S(t)^\dagger : b_j a_k : S(t) | \Phi_o \rangle \\ & + \langle \psi_j^{(-)} | L | \psi_k^{(-)} \rangle \langle \Phi_o | S(t)^\dagger : b_j b_k^\dagger : S(t) | \Phi_o \rangle \Big] \end{aligned} \tag{16}$$

where

$$L(x) = i\partial_t - h(x), \quad h(x) = \vec{\alpha}\cdot(-i\vec{\nabla}-\vec{A}) + \beta m + A_o \tag{17}$$

This representation of the action is almost normal ordered; only the last term need be changed. In order to evaluate Eq. (16), we need to calculate matrix elements of operators which have a form $S(t)^\dagger a_j^\dagger a_k S(t)$. This is carried out as follows. We expand the operators $\alpha_j(t)$ and $\beta_j^\dagger(t)$ as

$$\begin{aligned} \alpha_j(t) &= U_{jk}(t)a_k + V_{jk}(t)b_k^\dagger \\ \beta_j^\dagger(t) &= -V_{jk}(t)a_k + U_{jk}(t)b_k^\dagger, \end{aligned} \tag{18}$$

where all of the time dependence is contained in the expansion coefficients U(t) and V(t). Equation (18) represents the most general expansion which satisfies the anticommutation relations, Eq. (6), and the constraints of unitarity. The properties of the transformation (18) are more evident in the finite representation obtained by truncating the positive and negative continuum, as illustrated in Fig. 2. Thus for the operators, α_j and β_j are limited to $0 < j < N$ for α_j, and $-m < j < 0$ for β_j. In this truncated Hilbert space, Eq. (18) becomes an M+N dimensional unitary transformation of the vector comprised of the set of operators α_j and $\beta_j^\dagger$,

$$\begin{pmatrix} \alpha(t) \\ \beta^\dagger(t) \end{pmatrix} = \begin{pmatrix} U & V \\ -V & U \end{pmatrix} \begin{pmatrix} a \\ b^\dagger \end{pmatrix}, \tag{19}$$

where the elements of the transformation matrix are the expansion coefficients in Eq. (18). It is straightforward to invert Eq. (19) and obtain the matrix elements needed to evaluate the action. In matrix form these are

$$\begin{pmatrix} S^\dagger a S \\ S^\dagger b^\dagger S \end{pmatrix} = \begin{pmatrix} U^\dagger & -V^\dagger \\ V^\dagger & U^\dagger \end{pmatrix} \begin{pmatrix} a \\ b^\dagger \end{pmatrix}. \tag{20}$$

The norm of the vector in Eqs. (19) and (20) is invariant under the finite rank transformation (19)

$$\begin{aligned} N &= (a^\dagger b) \begin{pmatrix} a \\ b^\dagger \end{pmatrix} \\ &= a_j^\dagger a_j + b_j b_j^\dagger, \end{aligned} \tag{21}$$

and thus is a constant of the motion. Equation (19) differs from the lepton number only by a time-independent constant, and hence gives lepton number conservation.

In this treatment, the matrix of coefficients U(t) and V(t) are unknown variational parameters which are determined by finding stationary values of the action

$$\delta S/\delta U = \delta S/\delta V = 0. \tag{22}$$

These yield equations of motion

$$h \left| \psi_q^{(s)}(t) \right\rangle = i\partial_t \left| \psi_q^{(s)}(t) \right\rangle,$$

for

$$\left| \psi_q^{(+)}(t) \right\rangle = U^*_{qk}(t) \left| \chi_k^{(+)} \right\rangle + V^*_{qk}(t) \left| \chi_k^{(-)} \right\rangle \quad q < f \tag{23}$$

and

$$\left| \psi_q^{(-)}(t) \right\rangle = -V^*_{kq}(t) \left| \chi_k^{(+)} \right\rangle + U^*_{kq}(t) \left| \chi_k^{(-)} \right\rangle \quad q < 0$$

where h is given by Eq. (17). Classical field equations are obtained in a similar way

$$\delta S/\delta A^{\nu} = 0, \tag{24}$$

and result in the usual Maxwell's equations

$$\partial^{\mu} F_{\mu\nu} = J_{\nu} + \langle \Phi(t) \left| : \bar{\psi}(x)\gamma_{\nu}\psi(x): \right| \Phi(t) \rangle \tag{25}$$

where the current matrix element is evaluated using the methods outlined above. Equations (23) and (25) comprise Dirac-Hartree equations for a set of orbitals, which may be solved without explicit reference to the U and V matrices.

BASIS SPLINE EXPANSION

In this section we shall address a method of solving Eqs. (23) using the basis spline collocation method. Full details of this technique are given in Ref. 4. For simplicity, we shall consider the one-dimensional Dirac equation as given below,

$$h_o \psi(x,t) = i\partial_t \psi(x,t) \tag{26}$$

where the Hamiltonian is spin-degenerate, so that it suffices to specify h in a two-component spinor representation as

$$\begin{aligned} h &= \alpha_x \left(-i\partial_x - A_x\right) + \beta m + A_o \\ &= \begin{bmatrix} A_o + m & -i\partial_x - A_x \\ -i\partial_x - A_x & A_o - m \end{bmatrix} \end{aligned} \tag{27}$$

We shall assume that the field equations, Eq. (25), are integrable and develop numerical methods of solving Eq. (26) which emphasize accuracy, stability, and ease of programming. Our method requires the expansion of the spinor in Eq. (26) on a basis of spline functions[8] of order N,

$$\psi(x) = U_k^N(x)\psi^k, \quad k = 1,\ldots,n, \tag{28}$$

where we shall use the convention that repeated indices are summed. Splines of order N are piecewise $(N-1)^{th}$ differentiable polynomials, for which the index k is associated with some space interval. Examples of these functions are shown in Fig. 3. Since the number of B-splines in Eq. (28) is finite, they cover a finite interval. In a completely different context, calculations using B-splines have been given by Dreizler.[9] The set of space points X_k, associated with the spline functions, U_k^N, do not provide an adequate representation for operators of the form Eq. (27). There are three problems which must be addressed: i) finding a local representation that sidesteps the issue of constructing matrix elements of h by numerical integration; ii) representing the derivatives on the spinors so that the boundary conditions on the upper and the lower components are correct; and iii) satisfying current conservation conditions on the space lattice that are implicitly contained in the Dirac Hamiltonian. The latter point is, of course, essential to guarantee lepton number conservation in numerical calculations.

There are a set of space points associated with each spline function which minimizes the error in the expansion, Eq. (28). These points, ξ_α $\alpha = 1,\ldots,n$, called collocation points, provide an optimal representation of a function on a finite interval. The set of collocations may be evaluated using several different methods;[8,10] however, for equally spaced points x_k, $k = 1,\ldots n$, we may take

$$\xi_\alpha = \left(X_{\alpha+\mu} + X_{\alpha+\mu+1}\right)/2 \quad \mu = [N/2]. \tag{29}$$

These points are shown as the open circles in Fig. 3. Thus, the functions Ψ evaluated at ξ_α are given by the transformation

$$\psi_\alpha = B_{\alpha k}\,\psi^k, \tag{30}$$

with

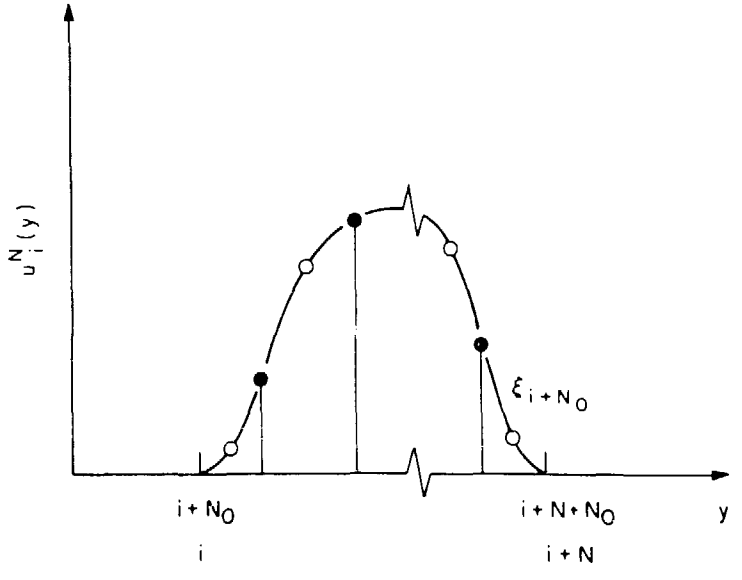

Fig. 3

$$B_{\alpha k} = U_k^N(\xi_\alpha).$$

For B-splines of finite order, the matrix B is banded with a bandwidth of N. Also, the inverse transformation is well behaved, thus giving the coefficient of ψ^k in terms of ψ_α,

$$\psi^k = B^{k\alpha}\,\psi_\alpha,$$
$$B^{k\alpha} = [B^{-1}]^{k\alpha}. \tag{31}$$

Representations of differential operators can be easily obtained as matrices in collocation space; for example, $\partial_x^2 = \Delta$ becomes

$$\Delta_\alpha^{\ \beta} \equiv B''_{k\alpha}\, B^{k\beta},$$
$$B''_{k\alpha} = \partial_x^2\, U_k^N(x)\Big|_{x\,=\,\xi_\alpha}, \tag{32}$$

where the matrix $B^{k\beta}$ plays the role of a metric in collocation space. Equation (32) yields a highly accurate representation of the second derivative operator on a lattice, as illustrated in Fig. 4, where we give the result of the matrix Δ acting on the vector f(q)

$$F_2(q) = \Delta f(q)$$
$$f(q) = \frac{\cos(q\xi_\alpha)}{-q^2}. \tag{33}$$

In Fig. 4 $\xi_\alpha = 0$, so that F_2 should take on a constant value, one. We compare the results of the ordinary finite-difference method, dashed curve, with the two B-spline results of order 3 and 11, as a function of q. The B-spline results are clearly superior, and, in general, for B-splines of order N, and for n collocation points, the error in the representation Eq. (32) is

$$\text{error} \sim n^{-N+1}. \tag{34}$$

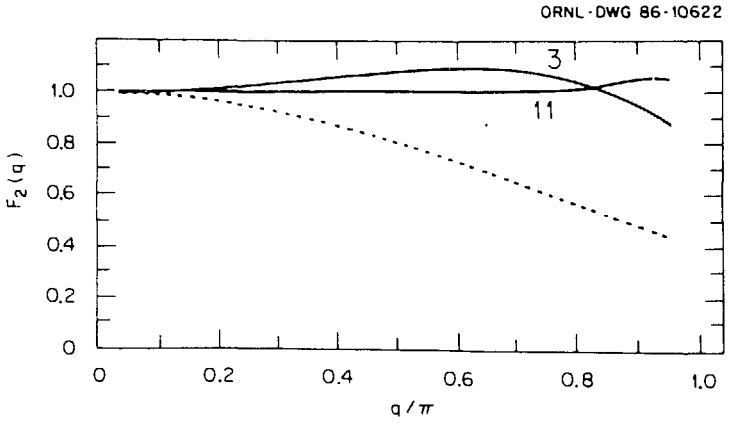

Fig. 4

This form of the second derivative operator has a unique decomposition into upper and lower triangular form using the Cholesky decomposition,[11]

$$\Delta = D^- D^+, \tag{35}$$

where in Eq. (35) D^- is a lower and D^+ is an upper triangular matrix, and where we have imposed the condition

$$D^-_{\alpha\alpha} = \left| D^+_{\alpha\alpha} \right| \tag{36}$$

in order to achieve uniqueness. In this decomposition, we identify two types of first derivatives in which boundary conditions at ξ_1 are contained in D^+ and boundary conditions at ξ_n are contained in D^-. This decomposition has two important consequences for the Hamiltonian, Eq. (27). It resolves the problem of fermion doubling on the lattice,[12,13] and it maintains an exact current conservation on the lattice. Thus, the representation of Eq. (27) on a collocation lattice is

$$h = \begin{bmatrix} A_o + m & -iD^+ - A_x \\ -iD^- - A_x & A_o - m \end{bmatrix}, \tag{37}$$

where the potentials are local functions of space

$$\left(A_\mu\right)_\alpha^{\ \beta} = \delta_{\alpha\beta} A_\mu(\xi_\alpha). \tag{38}$$

Thus, Eq. (26) on the collocation lattice becomes

$$h_\alpha^{\ \beta} \psi_\beta(t) = i\partial_t \psi_\alpha(t). \tag{39}$$

A more extensive discussion of this method is given in Ref. 4; here we shall employ these techniques to study μ- and τ-pair production from the vacuum.

TRANSVERSE FIELD MODEL FOR PAIR PRODUCTION

In the collisions of two relativistic nuclei, the transverse, near-zone, electromagnetic field becomes very large. For two beams of uranium each at an energy per nucleon of 100 GeV, Gould[2] estimates μ-pair and τ-pair cross sections, respectively

$$\sigma_{\mu^+\mu^-} \sim 1 \text{ mb}$$

$$\sigma_{\tau^+\tau^-} \sim 1 \ \mu\text{b}.$$

These estimates are based on a perturbative treatment of the production, which is equivalent to the production out of the field of a time-like virtual photon that subsequently pair decays. However, these considerations suggest that the QED vacuum must undergo large rearrangements near such heavy ions. In the case of real photons coupled to static fields,[14] the dimensionless parameter which sets the scale for pair production, κ, is

$$\kappa = \left(\frac{\omega}{m}\right)\left(E/E_o\right) \tag{40}$$

where ω is the frequency of the photon field, m is the mass of the lepton, E is electric field strength, and E_o is the critical field,

$$E_o = m^2/e.$$

For μ and τ leptons, pair production becomes large whenever $\omega \approx m$, and $E \approx E_o$, as given below

	E_o (MV/fm)	ω^{-1} (fm/c)
μ	60	1.85
τ	15×10^3	0.1

Thus, if the transverse fields near the heavy ions have strengths and frequency components similar to these, we expect to observe sizeable amounts of pair production.

If we consider hadronic mechanisms for producing lepton pairs, we can get an idea as to the cross section scales. At these relativistic velocities, the Drell-Yan[15] mechanism sets the scale for the production, as shown in Fig. 5. Here the hard scattering of quark anti-quark pairs annihilate to give a time-like photon which pair decays. The total cross section for μ-pair production is approximately[16]

$$\sigma_{\mu^+\mu^-} \sim \frac{1.3\ A^{5/3}}{4\ M_\mu^{\ 2}}\ (\mathrm{fm}^2),$$

which for uranium collisions at 100 GeV per nucleon, gives

$$\sigma_{\mu^+\mu^-} \sim 1\ \mathrm{mb}$$

and about

$$\sigma_{\tau^+\tau^-} \sim 1\ \mu\mathrm{b}.$$

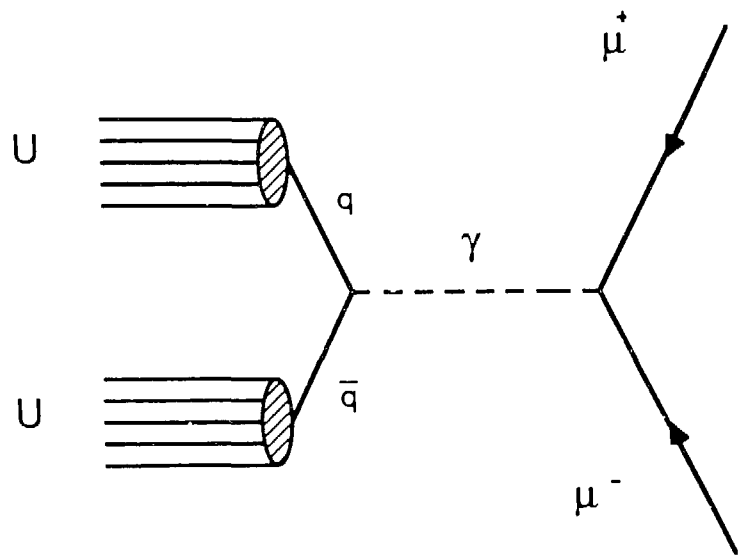

Fig. 5

These cross sections are comparable to those of Gould for the vacuum production of such pairs. The number of electron pairs produced in the heavy-ion collision is approximately 10^2 b; these pairs can convert to μ-pairs via the process shown in Fig. 1, which result in a production cross section of

$$\sigma_{e^+e^-\to\mu^+\mu^-} \sim 10^2 \text{ nb}.$$

Thus from these considerations, we conclude that excitations out of the QED vacuum near such heavy-ion beams are at least as large as other processes. For a heavy-ion collision as shown in Fig. 6, the near zone, transverse field a distance b from the beam axis is

$$E_\perp = \frac{Ze\gamma b}{\left(b^2+\beta^2 t^2\right)^{3/2}} ,$$

this field is shown schematically in Fig. 6. Note that the maximum field strength is simply $Ze\gamma/b^2$ and that, due to causality, it has an approximate width

$$\Delta t \sim b/\gamma\beta.$$

These parameters are given below for two combinations of heavy-ion beams, and for b = 10 fm.

γ	$E_\perp$ (MV/fm)	Δt (fm/c)
17	25	0.6
10×10^3	30×10^3	5×10^{-4}

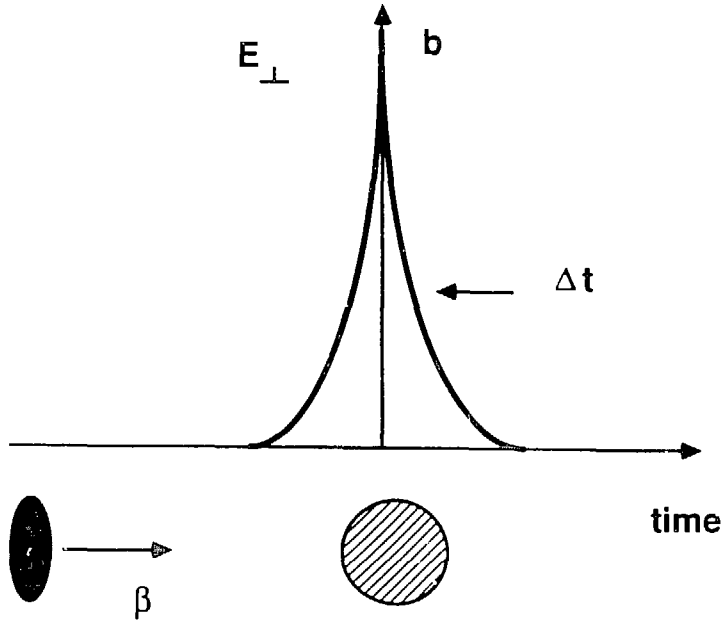

Fig. 6

The case of $\gamma = 17$ corresponds to the type of beams that will be available at the Brookhaven AGS shortly, and the case $\gamma = 20 \times 10^3$ corresponds to the proposed fixed target equivalent energy at RHIC. At AGS energies the field strength is 40% of the critical field for μ-pair production, and at RHIC energies it is 500 times the critical field. Hence, both of these machines should produce sizeable numbers of μ-pairs. At RHIC energies, we see that the field strength is twice the critical field for τ-pair production.

The excitation of such pairs out of the vacuum can be studied with a one-dimensional model as follows. Consider a box of length L in one-dimension, and a time-dependent electric field which is uniform throughout the box,

$$E(x,t) = E_o\, e^{-t^2/\Delta t^2} \tag{41}$$

The size of the box, the values of E_o, and the time history of the field are fixed to reproduce the values of the transverse field as previously discussed, so the E_o and Δt are functions of (γ,b). We shall only consider vacuum states and ignore binding effects so that the states in the box represent equivalent positive and negative energy continuum states. We shall use 74 positive energy and 74 negative energy continuum states and calculate the evolution of the vacuum, Eq. (23), using Eq. (41). Note that (41) is gauge equivalent to the interaction,

$$\begin{aligned} A_x &= 0, \\ A_o &= xE(t), \end{aligned} \tag{42}$$

which are used in the actual calculations. From Eq. (23), the vacuum evolution is obtained by time evolving all of the states $\psi_q^{(-)}$ with $-\nu < q < 0$. The truncation of the states in the vacuum to $q > -\nu$ is under our control and permits us to construct the density of states in the vacuum, evolve it in time, and examine its convergence properties. For example, the lowest energy state in the box has an energy $E_{-M} \sim -250\ mc^2$, whereas the density of states is usually cut off at about $E_\nu \sim -5\ mc^2$. With the wavefunction given by

$$|\, \psi_q^{(-)}(t)\rangle = -V_{kq}^*(t)\,|\, \chi_k^{(+)}\rangle + U_{kq}^*(t)\,|\, \chi_k^{(-)}\rangle,$$

there are three quantities of interest which can be constructed from the projections,

$$P_k^s = \sum_{-\nu<q<0} |\, \langle \chi_k^{(s)}\,|\, \psi_q^{(-)}\rangle\,|^2. \tag{43}$$

These are the inclusive spectra of emitted particles, $\overline{dp}/dE_k$, the density of states in the vacuum $\rho(\overline{\varepsilon_k})$, and the total probability density of producing a pair, $\omega(\gamma,b)$, given respectively as

$$\begin{aligned} \overline{dp}/d\varepsilon_k &= \overline{P}_k^{(+)}/\Delta E_k, \\ \rho(\overline{\varepsilon}_k) &= \overline{P}_k^{(-)}/\Delta E_k, \\ \omega(\gamma,b) &= \sum_k \overline{P}_k^{(+)}, \end{aligned} \tag{44}$$

where

$$\bar{p}_k^{(s)} = p_{k+1}^{(s)} + p_k^{(s)} \ldots /2,$$

and

$$\Delta E_k = | \varepsilon_{k+1} | - | \varepsilon_k | .$$

A typical example of the vacuum evolution is shown in Figs. 7-10 for the case of τ-pair production 15 fm from colliding beams of 50 GeV per nucleon uranium. In natural units, $\hbar = c = m = e = 1$, this would correspond to field strengths of 0.2 and a time width of 1.0. In these calculations, the lepton number is conserved to better than $1:10^{10}$. Figure 7 shows the pair production probability as a function of time. Here the time scale t_o is the Compton time of the tau, approximately

$$t_o \sim 10^{-24} \text{ sec.}$$

Note that the final pair multiplicity is about 10^{-2}, which is moderately large, and the sharp rise and subsequent fall of the probability in time, indicating rearrangement of the vacuum. Associated with this production probability is the inclusive τ^- spectra shown in Fig. 8. Here the differential probability, in units of the τ mass, is shown as a function of the kinetic energy of the τ^-, also in units of the τ mass. The dashed curves denote the contribution to the spectra from the individual states comprising the vacuum. In this example, we are propagating 12 states, and most of the yield occurs at kinetic energies less than the τ-mass. It is instructive to examine the density of states in the vacuum during the initial phase of the evolution, Fig. 9, and at the end of the time evolution, Fig. 10. Note that the ordinate scales for these figures are logarithmic, and hence the initial density of states is approximately $1/\Delta E_k$ for energies less than

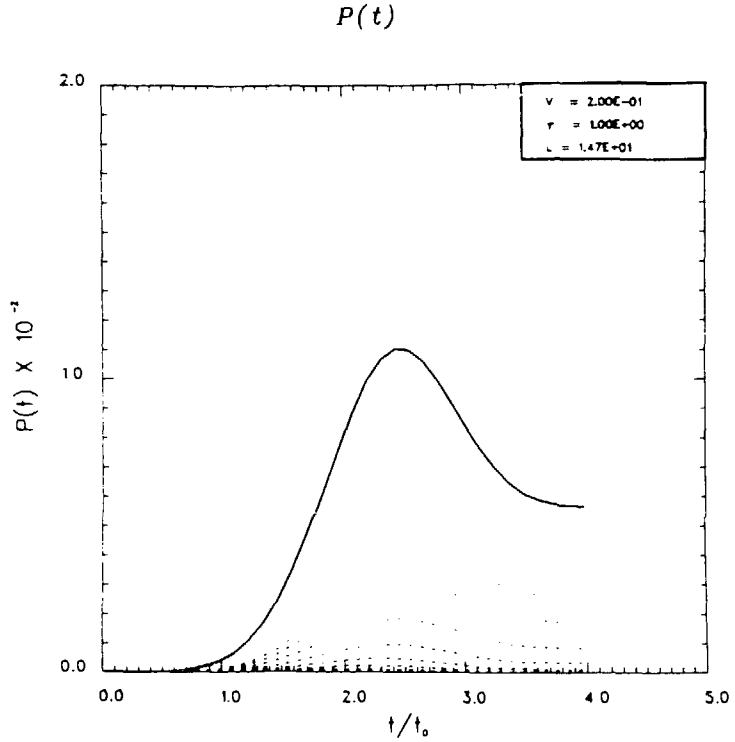

Fig. 7

Tauon Pair Spectrum $t/t_o = 3.985$

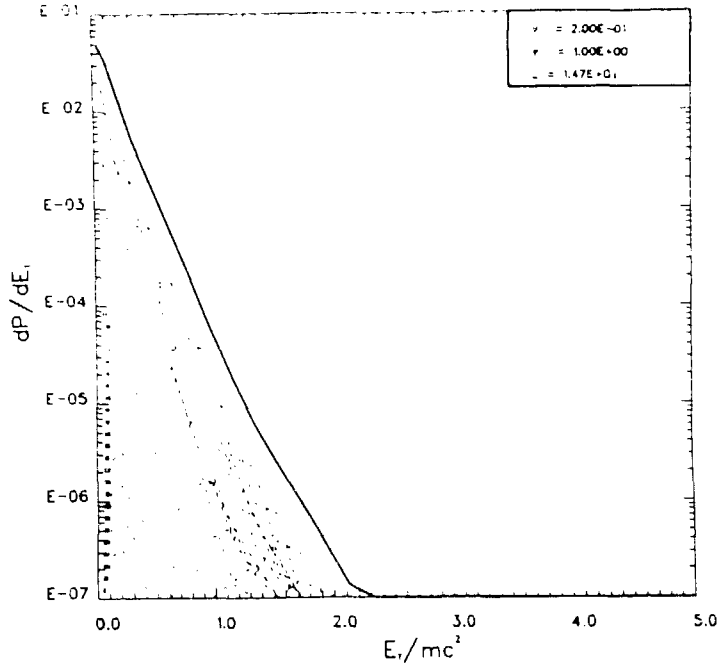

Fig. 8

Time Evolved Vacuum $t/t_o = 0.625$

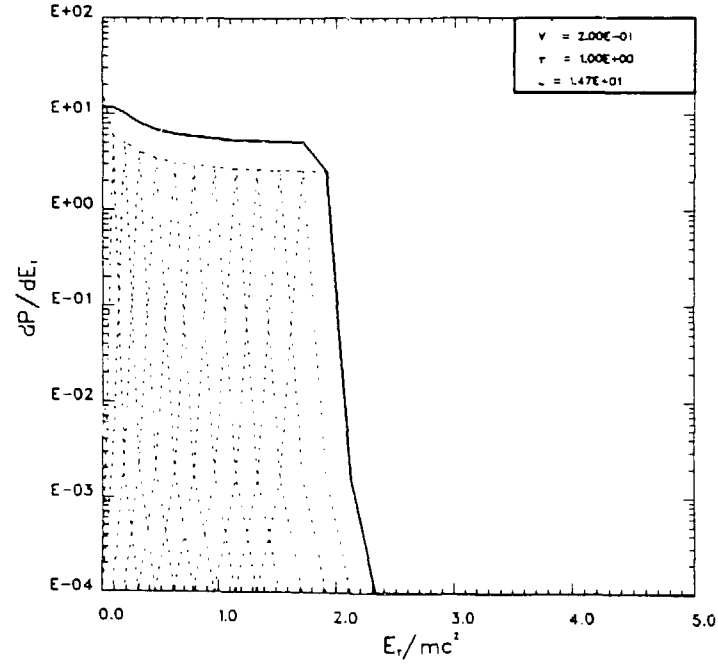

Fig. 9

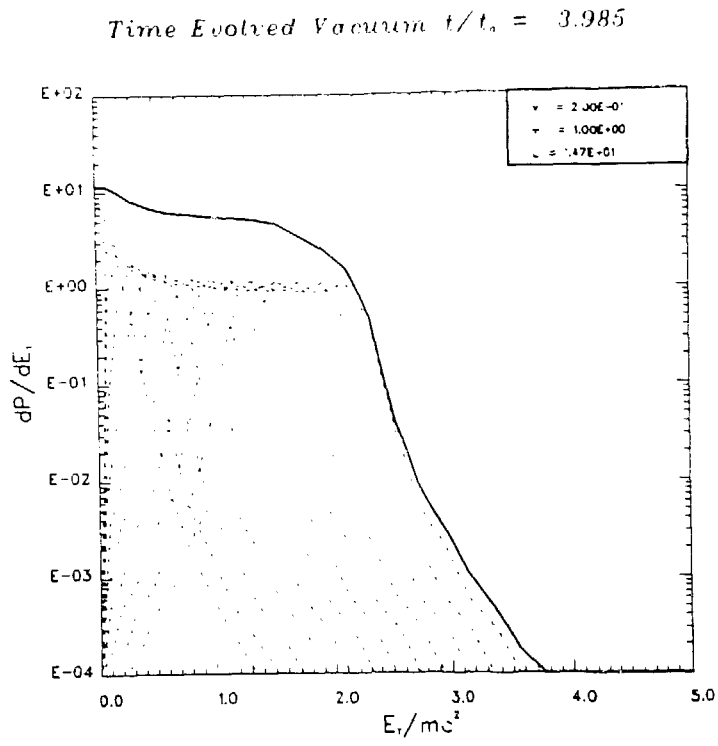

Fig. 10

about 2 mc^2, and zero for energies greater than 2 mc^2, while at the end of the evolution, there is considerable rearrangement of this function with an exponential falloff up to about 4 mc^2.

We can approximately reconstruct production cross sections from the observed probability density. In the above example, $P \sim 3.6 \times 10^{-3}$ yields, $\omega = 4 \times 10^{-3}$ fm^{-1} over a region of space of approximately 15 fm. Using a simple geometrical argument, the emission probability transversed to the heavy-ion beam times the transverse area would result in

$$\sigma \sim b^4 \omega^2 \tag{45}$$

where b is the impact parameter. Thus for 50 GeV per nucleon uranium beams,

$$\sigma_{\tau^+\tau^-} \sim 6 \text{ mb}.$$

Similar calculations for μ-pairs result in

E/A (GeV)	ω (fm^{-1})	σ (mb)
21	4×10^{-4}	.08
10^2	5×10^{-3}	12

In summary, we conclude that the near-zone electromagnetic field in relativistic heavy-ion collisions produces large changes in the QED vacuum which have characteristically large Fourier frequency components. This is reflected in the sizeable emission of heavy leptons in a direction transverse to the heavy-ion beam.

REFERENCES

1. C. Bottcher and M. R. Strayer, in: "Procs. of the Atomic Theory Workshop and QED Effects in Heavy Atoms," National Bureau of Standards, 1985.
2. H. Gould, in: "Procs. of the Atomic Theory Workshop and QED Effects in Heavy Atoms," National Bureau of Standards, 1985.
3. J. Reinhardt and W. Greiner, in: "Heavy-Ion Science," D. Allan Bromley, ed., Plenum Press, New York (1985).
4. C. Bottcher and M. R. Strayer, submitted to Annals of Physics (N.Y.), June 1985.
5. C. Itzykson and J. B. Zuber, "Quantum Field," McGraw-Hill, New York, (1980).
6. J. W. Negele, Revs. Mod. Phys. 54:913 (1982).
7. A. K. Kerman and S. E. Koonin, Ann. Phys. (N.Y.) 100:332 (1976).
8. C. de Boor, "A Practical Guide to Splines," Springer-Verlag, New York (1978).
9. R. Dreizler, Z. Physik A309:5 (1982); ibid., A307:211 (1982).
10. U. Asher, J. Computational Phys. 34:401 (1980).
11. V. Vemuri and W. J. Karplus, "Digital Computer Treatment of Partial Differential Equations," Prentice-Hall, New York (1981).
12. C. Bottcher and M. R. Strayer, Phys. Rev. Lett. 54:669 (1985).
13. C. M. Bender, K. A. Milton, and D. H. Sharp, Phys. Rev. D31:383 (1985).
14. V. N. Bair, V. M. Katkov, and V. M. Strakhovenko, Nucl. Instr. and Meth. B16:5 (1986).
15. R. C. Hwa and K. Kajantie, Phys. Rev. D32:1109 (1985).
16. M. Gyulassy, private communication.